Supplementary Information

Surface stabilities and NO oxidation kinetics on hexagonal-phase $LaCoO_3$ facets: a first-principles study

Xiao Liu,[a,b] Zhengzheng Chen,[b] Yanwei Wen,[b] Rong Chen,*[a] Bin Shan*[b,c]

[a] *State Key Laboratory of Digital Manufacturing Equipment and Technology and School of Mechanical Science and Engineering, Huazhong University of Science and Technology, Wuhan 430074, Hubei, People's Republic of China*

[b] *State Key Laboratory of Material Processing and Die and Mould Technology and School of Materials Science and Engineering, Huazhong University of Science and Technology, Wuhan 430074, Hubei, People's Republic of China*

[c] *Department of Materials Science and Engineering, The University of Texas at Dallas, Richardson, Texas 75080, USA*

*Corresponding authors: bshan@mail.hust.edu.cn (Bin Shan), rongchen@mail.hust.edu.cn (Rong Chen)

Corresponding relationships between cubic and hexagonal $LaCoO_3$

The symmetry of cubic $LaCoO_3$ is $Pm\bar{3}m$ (space group number 221). Typical low index crystalline direction families are <100>, <110> and <111>, which have 6, 12 and 8 equivalent directions, respectively. The corresponding crystal planes of three direction families are shown in Figure S1. Referring to the surface structure, we have found the corresponding crystal directions in hexagonal phase, the symmetry of which is $R\bar{3}c$ (space group number 167).

As shown in Figure S2, the surface structure of $\{1\bar{1}02\}$ in hexagonal $LaCoO_3$ are similar to {100} (Figure S1(a)), which means 6 $<1\bar{1}02>$ directions are corresponding to 6 <100> directions in cubic phase. It is evident that oxygen atoms have slight displacement from the cubic lattice because of Jahn-Teller distortion which is the main difference between cubic and hexagonal $LaCoO_3$. Similarly in Figure S3 and Figure S4, the surface structure of $\{11\bar{2}0\}$ and $\{\bar{1}104\}$ in hexagonal $LaCoO_3$ are corresponding to {110} (Figure S1(b)), and the surface structure of {0001} and $\{\bar{1}101\}$ are similar to {111} (Figure S1(c)). As the special low index crystal planes, we also have considered $\{10\bar{1}0\}$ shown in Figure S5.

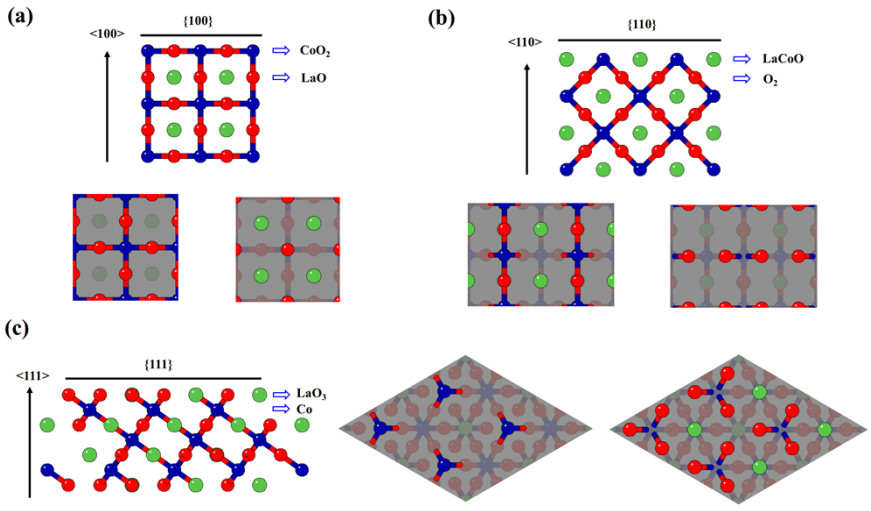

Figure S1. The side view of (a) {100} (b) {110} and (c) {111} of cubic $LaCoO_3$. The dark shadows are their surface structure with different terminations.

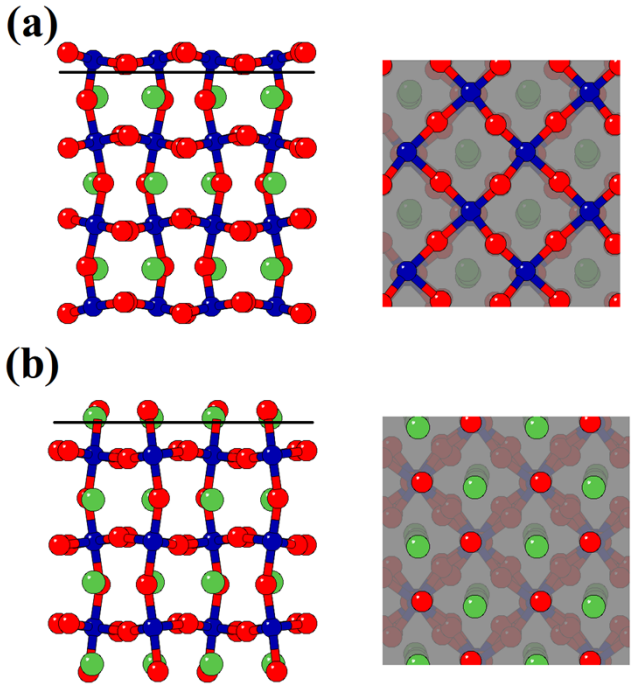

Figure S2. The side and top view of optimized (a) $(1\bar{1}02)$-CoO_2 and (b) $(1\bar{1}02)$-LaO slabs.

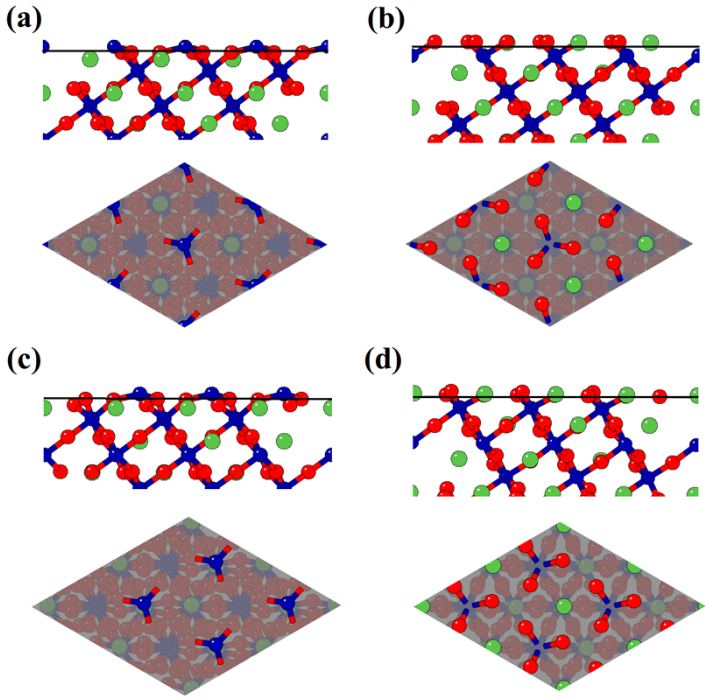

Figure S3. The side and top view of optimized (a), (b) (0001)-Co, -LaO_3 and (c), (d) ($\bar{1}101$)-Co, -LaO_3

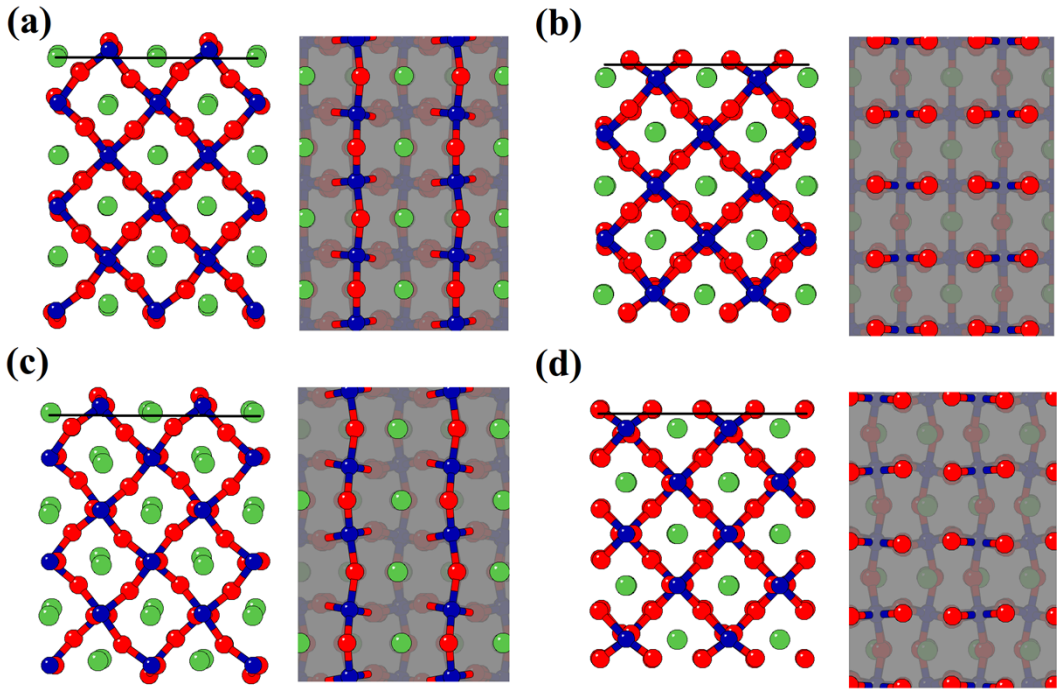

Figure S4. The side and top view of optimized (a), (b) $(11\bar{2}0)$-LaCoO, -O_2 and (c), (d) $(\bar{1}104)$-LaCoO, -O_2.

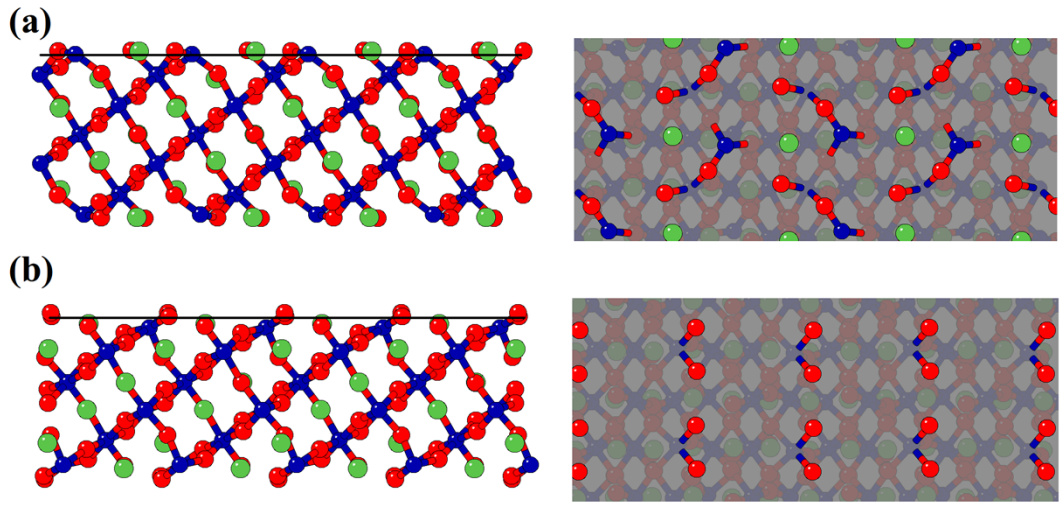

Figure S5. The side and top view of optimized (a) $(10\bar{1}0)$-LaCoO and (b) $(10\bar{1}0)$-O_2 slabs.

Surface structures with reconstruction

As shown in Figure S6, $p(2\times1)$, $p(2\times2)$, $c(2\times1)$ and $c(2\times2)$ are all 1/2 reconstruction, which remove half charges of up and down surface to reduce polarization and surface energy. $p(2\times1)$ and $p(2\times2)$ will remove half atoms per formula unit O_2 which is the unit cell of the surface.[1] $c(2\times1)$ and $c(2\times2)$ will remove single oxygen atom.[2] For $p(2\times1)$ and $c(2\times1)$, the remained atoms in reconstructed surface are in lines. However, the remained atoms are zigzag arrangement for $p(2\times2)$ and $c(2\times2)$.

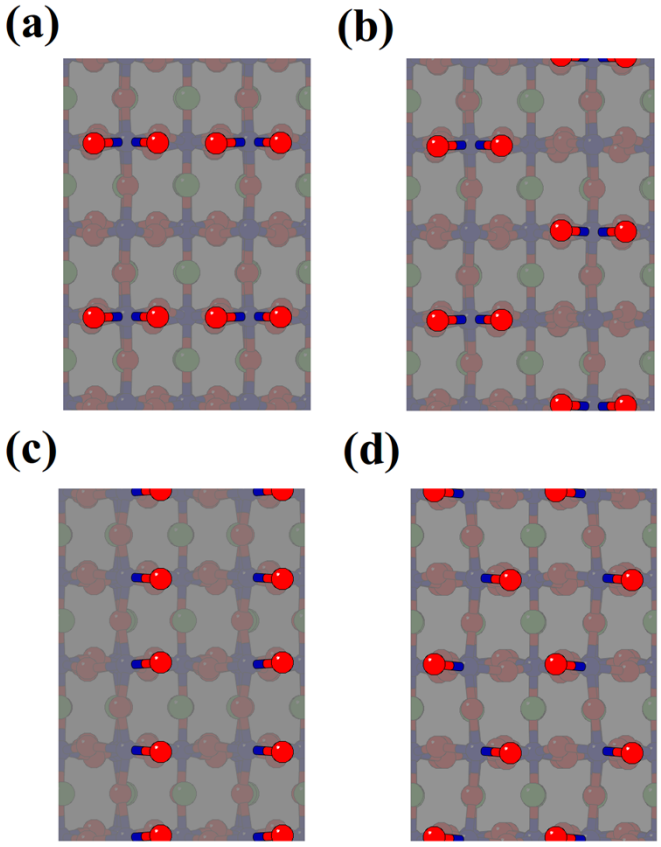

Figure S6. The top view of $(11\bar{2}0)$-O_2 with (a) $p(2\times1)$, (b) $p(2\times2)$, (c) $c(2\times1)$ and (d) $c(2\times2)$ reconstruction.

Grand surface energy and stoichiometric ratio

Table S1 has listed the grand surface energy at $\Delta\mu_{Co} = \Delta\mu_O = 0$ eV (Ω_0) and the stoichiometric ratio of the slabs, where $\Delta\mu_{Co} = \mu_{Co} - \mu_{Co}^0$ and $\Delta\mu_O = \mu_O - \mu_O^0$. Based on these data and formula (2) in article, we can plot the relationship between the grand surface energy (Ω) and $\Delta\mu_{Co}$, $\Delta\mu_O$ and get Figure 3(a).

Table S1. Data about the grand surface energy at $\Delta\mu_{Co} = \Delta\mu_O = 0$ eV (Ω_0) and the stoichiometric ratio of the slabs.

Surface		Ω_0 (J/m^2)	N_{La}	N_{Co}	N_O
(0001)-Co	*p*11	2.4787	6	7	18
	*p*21	1.3109	12	12	36
	*p*22	1.3097	24	24	72
(0001)-LaO_3	*p*11	1.2463	7	6	21
	*p*21	1.6580	12	12	36
	*p*22	2.1159	24	24	72
$(\bar{1}101)$-Co	*p*11	2.4815	6	7	18
	*p*21	1.3844	12	12	36
	*p*22	1.3237	24	24	72
$(\bar{1}101)$-LaO_3	*p*11	1.2698	7	6	21
	*p*21	1.7237	12	12	36
	*p*22	2.2205	24	24	72
$(1\bar{1}02)$-CoO_2	*p*11	1.3532	6	8	22
	*p*21	1.8715	12	12	36
	*p*22	1.3122	24	24	72
$(1\bar{1}02)$-LaO	*p*11	1.8842	8	6	20
	*p*21	1.8949	12	12	36
	*p*22	2.2555	24	24	72
$(10\bar{1}0)$-LaCoO	*p*11	2.7087	14	14	38
	*p*21	1.4864	24	24	72
	*p*22	1.5696	48	48	144
$(10\bar{1}0)$-O_2	*p*11	1.4186	12	12	40
	*p*21	1.6735	24	24	72
	*p*22	1.4602	48	48	144
	*c*21	1.4313	12	12	36
	*c*22	1.3585	12	12	36
$(11\bar{2}0)$-LaCoO	*p*11	3.8683	12	12	32
	*p*21	1.6945	20	20	60
	*p*22	1.7705	40	40	120

$(11\bar{2}0)$-O_2	$p11$	1.1924	10	10	34
	$p21$	1.4913	20	20	60
	$p22$	1.5174	40	40	120
	$c21$	1.1606	10	10	30
	$c22$	1.1563	10	10	30
$(\bar{1}104)$-LaCoO	$p11$	3.8683	12	12	32
	$p21$	1.6945	20	20	60
	$p22$	1.7705	40	40	120
$(\bar{1}104)$-O_2	$p11$	1.1924	10	10	34
	$p21$	1.4913	20	20	60
	$p22$	1.5174	40	40	120
	$c21$	1.1397	10	10	30
	$c22$	1.1370	10	10	30

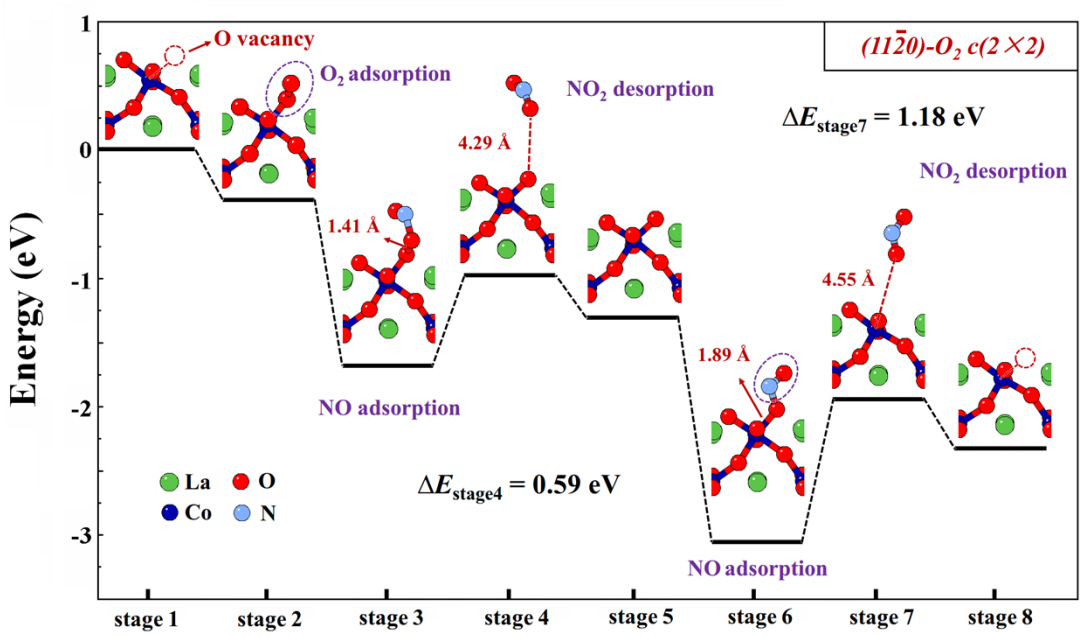

Figure S7. Energetic scenario of NO oxidation on (11$\bar{2}$0)-O_2 c(2×2) termination. The total reaction can be summarized as $2NO + O_2 \rightarrow 2NO_2$, exothermally.

Reference

1 C. Noguera, *J. Phys.: Conden. Matter*, 2000, **12**, R367.

2 F.Bechstedt, *Principles of Surface Physics*, Springer-Verlag, New York, 2003.